

# The Charge of Glass and Silica Surfaces

Sven H. Behrens and David G. Grier

*Dept. of Physics, James Franck Institute, and Institute for Biophysical Dynamics  
The University of Chicago, Chicago, IL 60637  
(May 30, 2018)*

We present a method of calculating the electric charge density of glass and silica surfaces in contact with aqueous electrolytes for two cases of practical relevance that are not amenable to standard techniques: surfaces of low specific area at low ionic strength and surfaces interacting strongly with a second anionic surface.

## I. INTRODUCTION

Ionization processes in aqueous solutions have long been a point of central interest to physical chemistry. Much progress has been made in recent years in understanding the charging properties of such different entities as small molecules, polyelectrolytes and various kinds of interfaces [1].

In this context, silica and silicate glass surfaces immersed in water are known to acquire a negative surface charge density, primarily through the dissociation of terminal silanol groups. The degree of dissociation and thus the surface charge density results from an equilibrium between counterions at the glass surface and free ions in the bulk electrolyte. Experimentally, this type of equilibrium and its dependence on the solution conditions can be studied by potentiometric acid-base titrations on colloidal dispersions of non-porous silica particles [2]. This technique actually measures the volume concentration of protons transferred between the surfaces and the solution. In order for the surfaces to accommodate a sufficient amount of charge, the electrostatic interaction between the surface sites must be screened at least partially by added salt ions, and/or the available surface area must be large.

These constraints can be relaxed to some degree by resorting to alternative techniques like microelectrophoresis [3,4], streaming potential measurements [5], conductometry [6] and electroacoustic methods [7,8]. All of these methods, however, rely heavily on approximate models for electrostatic or hydrodynamic processes in the interfacial region, introducing uncertainties that are difficult to estimate. We are not aware of any way to measure directly the surface charge of silica in a solution of very low ionic strength.

Theoretical studies of low ionic strength solutions typically deal with dense colloidal and macroionic systems and consider the regime of “no salt”, “low salt”, or “counterions only”. Here the defining assumption is that the overall ionic strength is due predominantly to the particles or macroions and the compensating counterions in solution, whereas the concentration of any additional ions is negligible. For colloidal dispersions this assumption is again legitimate if the specific surface area carrying the colloidal charge is large.

A series of recent experiments has spurred interest in the charge on glass and silica surfaces of low specific area in pure water, *i.e.* systems for which the usual picture of the “no salt” regime does not apply. For example, interaction measurements using digital video microscopy and optical trapping suggest that highly charged latex spheres may experience an anomalous long-ranged attraction when confined by charged glass walls [9–12], contrary to the predictions of Poisson-Boltzmann theory [13–15]. In one particular case [12], the attraction appears to result from a hydrodynamic interaction driven by the spheres’ electrostatic repulsion from a nearby wall [16]. This explanation hinges on the heretofore untested assumption that the glass wall carries an effective charge density of  $-2000 \pm 200 e/\mu\text{m}^2$ , where  $e$  is the elementary charge. Such hydrodynamic coupling cannot explain the like-charge attractions measured for spheres confined between two charged glass walls [9–11]. How the walls’ charge influence colloidal electrostatic interactions is not yet resolved, in part because of open questions regarding the charging state of the glass. We recently reported that the pair interaction of silica spheres remains monotonically repulsive even in the presence of a charged glass wall [17]. The spheres’ effective surface charge density of  $-700 \pm 150 e/\mu\text{m}^2$  extracted from these measurements is considerably smaller than the value posited in Ref. [16] for a compact glass surface.

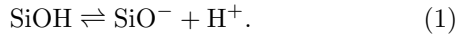
Because a silica surface’s charge density depends on the local chemical environment, it necessarily varies with proximity to other charge-carrying surfaces. The interpretation of typical particle deposition experiments [18] and force measurements by atomic force microscopy (AFM) [19,20] or total internal reflection microscopy (TIRM) [21] for example, is complicated by the fact that the charge densities of the substrate and the probe are a function of their separation, a phenomenon known as “charge regulation”. Since local properties of the enclosed solution rather than bulk properties determine the charging state, a naive use of charging data from bulk measurements can lead to errors.

In the following section we discuss how the experimentally supported 1-pK Basic Stern Model for silica surfaces may be used to calculate the elusive charge of glass plates and strongly diluted silica particles in deionized water. In the remainder of this paper we take advantage

of a recently proposed theoretical treatment of charge regulation [22,23] to discuss the charge of a silica-like surface in close proximity to a second anionic surface, which will be chosen, in view of the most common applications, as either of the same type or of constant charge (like sulfate latex) or of carboxylic nature (like carboxyl latex and many biological surfaces).

## II. EFFECTIVE CHARGE OF GLASS AND SILICA IN DEIONIZED SOLUTIONS

The principal mechanism by which glass and silica surfaces acquire a charge in contact with water is the dissociation of silanol groups [2]



Further protonation of the uncharged group is expected only under extremely acidic conditions [24,25] and will be disregarded. Similarly, we will not take into account the protonation of doubly coordinated  $\text{Si}_2 - \text{O}$  groups as these are generally considered inert [24].

In addition to the hydronium or other counterions dissociated from the surface, the bulk electrolyte also includes ions due to the autodissociation of water; the latter can dominate the concentration of mobile ions if the ratio of surface area to solution volume is exceedingly small. Under these conditions, the charging state of the surface is controlled by the ionic strength and pH of the bulk electrolyte, just as in the general case of high salt concentrations. We propose to take advantage of this similarity by applying insights gained from studies at high electrolyte concentrations to calculate the charge density at silica-water interfaces with low surface area and with no added salt.

Whether the specific surface area is indeed small enough to warrant a “high salt” treatment, depends largely on the geometry of the considered experimental setup and has to be checked on a case-by-case basis. For some of the aforementioned interaction measurements [12,17] this approach is appropriate, in other cases it may provide a very rough upper limit for the surface charge. If, on the other hand, the counterions due to the charged surfaces give a non-negligible contribution to the overall ionic strength, they have to be considered explicitly, for instance within a cell model [26,27]. Here, we concentrate on the former case of “high salt” and adopt the Basic Stern model [28], which has been shown to accurately describe titration data [29] obtained in the this regime for nominally nonporous, fully hydrated silica particles [24,25].

Within the Basic Stern model the charge of silica is regarded as localized entirely on the surface and arising from a concentration  $\Gamma_{\text{SiO}^-}$  of dissociated head groups

[22], giving rise to the surface charge density

$$\sigma = -e\Gamma_{\text{SiO}^-}. \quad (2)$$

Under normal conditions, only a fraction of the total concentration,

$$\Gamma = \Gamma_{\text{SiO}^-} + \Gamma_{\text{SiOH}}, \quad (3)$$

of chargeable sites dissociate. The relevant mass action law for the deprotonation reaction, Eq. (1),

$$\frac{[\text{H}^+]_0 \Gamma_{\text{SiO}^-}}{\Gamma_{\text{SiOH}}} = 10^{-\text{pK}} \text{ Mol/l}, \quad (4)$$

is characterized by the logarithmic dissociation constant, pK, and accounts for the influence of the surface’s electrostatic potential,  $\psi_0$ , through the surface activity of protons,

$$[\text{H}^+]_0 = [\text{H}^+]_b \exp(-\beta e \psi_0). \quad (5)$$

Here,  $[\text{H}^+]_b = 10^{-\text{pH}} \text{ Mol/l}$  is the bulk activity of protons, and  $\beta^{-1} = k_B T$  denotes the thermal energy. The dissociation constant is an inherent property of the silicate-water interface and is estimated to be  $\text{pK} = 7.5$  on the basis of a surface complexation model [24].

As counterions dissociate from the surface, they form a diffuse cloud of charge within the electrolyte. The Basic Stern model treats the counterions as being separated from the surface by a thin Stern layer across which the electrostatic potential drops linearly from its surface value,  $\psi_0$ , to a value  $\psi_d$  called the diffuse layer potential [28,22]. This potential drop is characterized by the Stern layer’s phenomenological capacity,

$$C = \frac{\sigma}{\psi_0 - \psi_d} \quad (6)$$

This capacity,  $C$ , reflects the structure of the silicate-water interface and should vary little with changes in surface geometry or electrolyte concentration. Titration data on colloidal silica [29] are consistent with  $C = 2.9 \text{ F/m}^2$  [24].

Eqs. (2–6) can be solved for the diffuse layer potential as a function of the charge density on the interface:

$$\psi_d(\sigma) = \frac{1}{\beta e} \ln \frac{-\sigma}{e\Gamma + \sigma} - (\text{pH} - \text{pK}) \frac{\ln 10}{\beta e} - \frac{\sigma}{C}. \quad (7)$$

This relation reflects the chemical nature of the interface and its charging process.

Another functional dependence follows from the distribution of mobile charges in the solution. If the latter is described by the Poisson-Boltzmann equation (PB), then the charge of an isolated, flat surface satisfies the Grahame equation

$$\sigma(\psi_d) = \frac{\varepsilon \kappa}{2\pi \beta e} \sinh\left(\frac{\beta e \psi_d}{2}\right). \quad (8)$$

Here,  $\varepsilon$  is the permittivity of the solution and  $\kappa^{-1}$  the Debye screening length given by  $\kappa^2 = 4\pi\beta e^2 n/\varepsilon$ , where  $n$  is the total concentration of small ions, all of which are assumed to be monovalent. The generalization of Eq. (8) to account for a curvature of radius  $a$ ,

$$\sigma(\psi_d) = \frac{\varepsilon\kappa}{2\pi\beta e} \left[ \sinh\left(\frac{\beta e\psi_d}{2}\right) + \frac{2}{\kappa a} \tanh\left(\frac{\beta e\psi_d}{4}\right) \right], \quad (9)$$

is known to give the surface charge density to within 5% for  $\kappa a \geq 0.5$  and any surface potential [30].

Combining Eq. (7) with Eq. (8) or (9) yields self-consistent values for the surface charge density,  $\sigma$ , and the diffuse layer potential,  $\psi_d$ . These values characterize the equilibrium of bound and mobile charges in the interfacial region, but are not necessarily accessible experimentally, given the requirement of large surface areas for potentiometric titrations and the interpretive ambiguities inherent to other techniques.

Most measurements of interfacial interactions probe the electrostatic potential  $\psi$  at distances for which  $e\psi \leq k_B T$ . Under these conditions  $\psi$  is described accurately by the linearized Poisson-Boltzmann equation, whose solution for a single flat surface has the form  $\psi(x) = \psi_{\text{eff}} \exp(-\kappa x)$ , where  $x$  is the distance from the surface. The effective surface potential  $\psi_{\text{eff}}$  in this experimentally accessible regime is related to the actual diffuse layer potential through [30]

$$\beta e\psi_{\text{eff}} = 4 \tanh\left(\frac{\beta e\psi_d}{4}\right). \quad (10)$$

Again, there is an approximate generalization for curved surfaces [31]:

$$\beta e\psi_{\text{eff}} = \frac{8 \tanh\left(\frac{\beta e\psi_d}{4}\right)}{1 + \left[1 - \frac{1+2\kappa a}{(1+\kappa a)^2} \tanh^2\left(\frac{\beta e\psi_d}{4}\right)\right]^{1/2}}. \quad (11)$$

The associated effective charge density can be obtained from

$$\sigma_{\text{eff}} = \frac{\varepsilon\kappa}{4\pi} \psi_{\text{eff}} \left[1 + \frac{1}{\kappa a}\right], \quad (12)$$

which is just the linearization of Eq. (9). This effective charge density characterizes essentially all of the recent measurements of electrostatic interactions between well-separated charged surfaces.

The effective charge's relevance to experimental observations is based in the popularity of the linear superposition approximation for estimating the interaction energy,  $u(h)$ , between two charged spheres of radii  $a_1$  and  $a_2$  as a function of their surface-to-surface separation  $h$ . In this approximation [32],

$$u(h) = \frac{1}{\varepsilon} \left( \frac{\sigma_1 a_1^2}{1 + \kappa a_1} \right) \left( \frac{\sigma_2 a_2^2}{1 + \kappa a_2} \right) \frac{\exp(-\kappa h)}{a_1 + a_2 + h}, \quad (13)$$

where  $\sigma_1$  and  $\sigma_2$  should be understood to be effective surface charge densities obtained from Eq. (11) rather than the bare charge densities from Eqs. (7) and (9). Using the effective surface charge densities implicitly accounts for overexponential decay of the electrostatic potential near the surfaces that follows from the nonlinearity of the Poisson-Boltzmann equation. The interaction between a sphere and a planar wall is obtained by taking the limit of one infinite radius in Eq. (13).

Fig. 1 shows computed values for the bare and effective charges of a planar silica surface and a 1  $\mu\text{m}$ -diameter silica sphere for pH values between 7 and the lowest pH compatible with an ionic strength of 1, 5, and 10  $\mu\text{Mol/l}$ . These are reasonable values for deionized water under usual experimental conditions. In addition to using  $C = 2.9 \text{ F/m}^2$  and  $\text{pK} = 7.5$ , we have further assumed a total site density of  $\Gamma = 8 \text{ nm}^{-2}$ , a commonly cited literature value for nonporous, fully hydrated silica [2]. Although  $\Gamma$  could vary widely depending on surface preparation, the degree of protonation is determined mostly by the electrostatic interactions among the small fraction of charged surface sites, rather than the large number of neutral sites that  $\Gamma$  accounts for, and so our results are quite insensitive to this parameter. This robustness validates our assumption that details in the structure of nonporous surfaces do not matter in the present context. Indeed, the top graph of Fig. 1 also should represent the charging properties of a polished glass surface. Note however that our arguments do not apply to some types of silica that are believed to be very porous and contain a much higher charge [2], the largest part of which seems located in the porous volume [33] rather than on the surface.

Fig. 1 demonstrates that the effective charge densities in deionized solutions do not depend as sensitively on pH as their “bare” counterparts, but that a significant variation with ionic strength persists. The top part of the figure indicates that the value of 2000 effective charges per  $\mu\text{m}^2$  ( $= -0.32 \text{ mC/m}^2$ ) assumed by Squires and Brenner [16] for a glass plate in contact with deionized solution of  $\kappa^{-1} = 0.275 \mu\text{m}$  (i.e. an ionic strength of  $1.2 \times 10^{-6} \text{ M}$ ) is very reasonable. The confirmation of this previously very uncertain value provides vital support for their recent electro-hydrodynamic explanation of apparent attractions between like-charged particles near a single glass wall.

In a study of the equilibrium interaction between few 1.58  $\mu\text{m}$  silica sphere at the bottom of a large glass container filled with deionized water, we found an ionic strength between  $8.5 \times 10^{-7}$  and  $1.1 \times 10^{-6} \text{ M}$  and a charge density between 550 and 830  $e/\mu\text{m}^2$  from a fit of measured interaction energies to Eq. (13) [17]. Comparison with Fig. 1 shows that these charge densities are a little below our expectation for isolated spheres, but have the right order of magnitude. The remaining difference can be explained by the spheres' close proximity to the

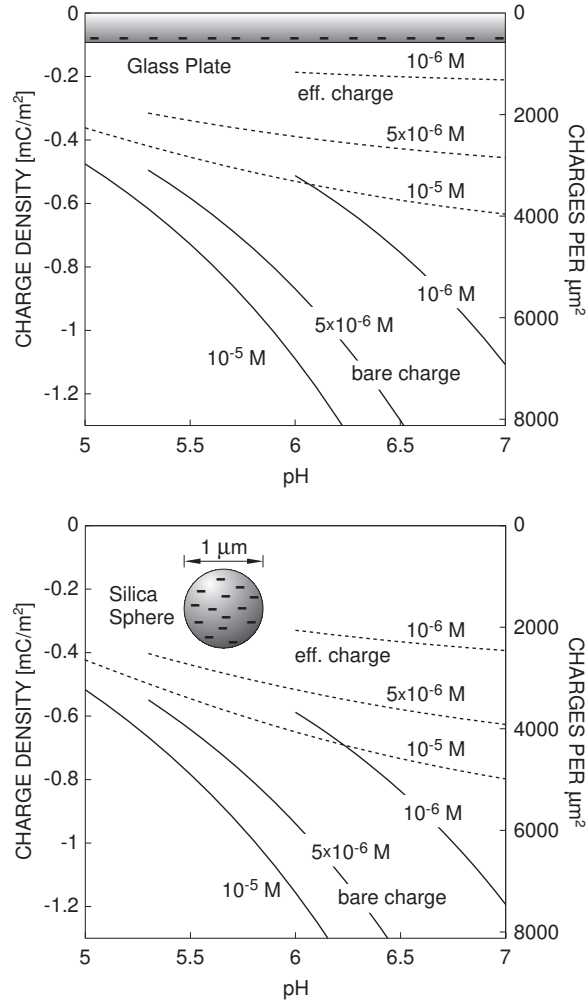


FIG. 1. The bare (full lines) and effective (dashed curves) charge densities of a planar glass wall and a 1 micron silica sphere, assuming a density  $\Gamma = 8 \text{ nm}^{-2}$  of chargeable sites, a pK value of 7.5 for the silanol dissociation, and a Stern capacity of  $2.9 \text{ F/m}^2$ .

bottom wall of the glass container, as we describe in the next section.

### III. CHARGE REGULATION OF ANIONIC SURFACES

Many experimental techniques to measure colloidal forces (AFM, TIRM, and the surface force apparatus, for instance) provide good resolution at very short distances. Often the surface separations  $h$  of interest are comparable to or smaller than the screening length and much smaller than the radii of curvature,  $a_1$  and  $a_2$ , of either surface. In this situation, the surfaces may be regarded as locally flat, and the Derjaguin approximation

$$f(h) = 2\pi \frac{a_1 a_2}{a_1 + a_2} W(h). \quad (14)$$

accurately expresses the magnitude  $f(h)$  of the acting force in terms of the interaction energy per unit area  $W(h)$  for two parallel (thick) plates of the same separation. This reduces the interaction problem to finding the energy  $W(h)$  or the dividing pressure  $\Pi(h) = -dW/dh$  resulting from a one-dimensional distribution of mediating small ions.

On the other hand, the superposition of the noninteracting surfaces' electrostatic potential is no longer warranted; nor can reliable results be expected from a solution of the *linearized* Poisson-Boltzmann equation, as it only captures the case of weak potentials (atypical for strongly interacting surfaces) or, with renormalized charges, the asymptotic behavior for large separations.

Instead, we consider the nonlinear PB equation, which in one dimension and for an excess of monovalent electrolyte ions reads

$$\frac{d^2 \Psi}{dx^2}(x) = \kappa^2 \sinh \Psi(x), \quad (15)$$

where  $\Psi = \beta e \psi$  is the dimensionless electrostatic potential and  $x$  the coordinate normal to the surfaces. Applying this mean field formalism to more general electrolytes shall not be discussed here, since neglected ion correlations and ion-specific interactions with the surfaces tend to complicate the case of polyvalent ions.

From Eq. (15) it is clear that  $\Psi(x)$  is a convex function for  $\Psi \leq 0$ . The charge density on either surface (1 or 2) is given, according to Gauss' law, by

$$\sigma_{1,2} = - \frac{\varepsilon}{4\pi\beta e z} \frac{d\Psi}{dx} \Big|_{1,2}, \quad (16)$$

where the derivative is taken at the surface with respect to its outward normal. It follows that between two negatively charged surfaces,  $\Psi(x)$  has a maximum  $\Psi_m$ , which for identical surfaces lies exactly at the midplane. Choosing generally the position of this maximum as the origin of our coordinate system (i.e.  $\Psi(0) = \Psi_m$ ), we can express the solution of Eq. (15) as [34,23]

$$\Psi(x) = \Psi_m + 2 \ln \text{cd}(u|m), \quad (17)$$

with

$$u = \frac{\kappa x}{2} \exp(-\Psi_m/2) \quad (18)$$

and

$$m = \exp(2\Psi_m), \quad (19)$$

where  $\text{cd}(u|m)$  is a Jacobian elliptic function of argument  $u$  and parameter  $m$  [35]. The derivative is

$$\frac{d\Psi}{dx} = \left(m^{3/4} - m^{-1/4}\right) \kappa \frac{\text{sn}(u|m)}{\text{cn}(u|m) \text{dn}(u|m)}, \quad (20)$$

where  $\text{sn}(u|m)$ ,  $\text{cn}(u|m)$ , and  $\text{dn} = \text{cn}/\text{cd}$  are again Jacobian elliptic functions of the argument  $u$  and parameter  $m$  given above. Efficient numeric implementations of these functions are readily available from mathematical libraries [36].

## Equal Surfaces

We shall measure the separation  $h$  between the surfaces by the distance between the head ends of the diffuse layer, i.e.,  $\Psi(h/2) = \beta e \psi_d$ . Evaluating Eqs. (16-20) at  $x = \pm h/2$  and combining them with the chemical boundary condition, Eq. (7), provides an expression for the actual surface charge density  $\sigma$ . The second boundary condition,  $d\Psi/dx = 0$  at  $x = 0$ , is already implied in the solution for  $\Psi(x)$ , Eq. (17). Note that for  $\sigma(\psi_d, h)$  defined by Eqs. (16) through (20), the long distance limit  $\lim_{h \rightarrow \infty} \sigma(\psi_d, h)$  is given by Eq. (8), which we have previously used for isolated surfaces and weakly interacting surfaces in the superposition approximation. In general,  $\sigma$  is a function of  $\psi_d$  as well as of the surface separation and cannot be expressed analytically. As before, the electrostatic definition of  $\sigma$ , Eqs. (16) and (20), depends parametrically on the Debye length, while the chemical definition, Eq. (7), depends only on pH and the surface chemical parameters,  $\Gamma$ , pK, and  $C$ .

Technically, the combination of Eqs. (7) and (16-20) results in a single transcendental equation for the mid-plane potential  $\Psi_m$ , whose numerical solution provides a very convenient alternative to numerical integration of the differential equation (15) with nonlinear boundary conditions.

Solving for  $\Psi_m$  has the further advantage of immediately yielding the electrostatic force per unit area

$$\Pi = nk_B T (\cosh \Psi_m - 1), \quad (21)$$

i.e. the excess osmotic pressure of small ions at the mid-plane where the electric field and the associated Maxwell stress are zero.

## Dissimilar Surfaces

The procedure described before may be applied to negatively charged surfaces other than glass or silica as long as the chemically imposed charge-potential relation  $\sigma(\psi_d)$  is modified to account for the surface properties of the considered material. Carboxylated latex for instance can be described in the same framework as silica, with a pK value of 4.9 for the dissociation of the carboxyl surface groups ( $\text{COOH} \rightleftharpoons \text{COO}^- + \text{H}^+$ ) and a large Stern capacity  $C$  (any value  $C \gg 10$  amounting to a negligible potential drop  $|\psi_0 - \psi_d|$  across the Stern layer) [37]. Sulfate latex, on the other hand, may be considered as having a constant charge density ( $\sigma(\psi_d) = -e\Gamma = \text{const.}$ ), because the strongly acidic sulfate groups are fully dissociated in all relevant solution conditions. Fig. 2 shows the predicted (and experimentally confirmed [24,37,38]) charging behavior of the aforementioned materials. The site density of  $\Gamma = 0.25 \text{ nm}^{-2}$  chosen for both the sulfate and the carboxyl surface lies in the typical range for

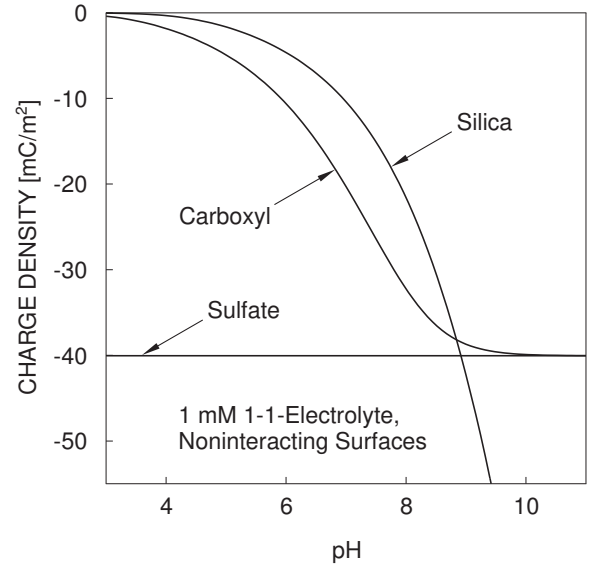


FIG. 2. The charge density of surfaces with silanol, carboxyl, or sulfate head groups as a function of pH. Parameters for the silica-like surface are as in Fig. 1. For both the sulfate- and the carboxyl bearing surface we have assumed a density  $\Gamma = 0.25 \text{ nm}^{-2}$  of sites, all of which are constantly charged in the sulfate case; further parameters of the carboxyl surface are a large (infinite) Stern capacity and a dissociation pK of 4.9.

commercially available latex spheres and has also been cited as the density of carboxyl groups on the membrane of blood cells [34].

A way to evaluate the interaction between two dissimilar surfaces starts by applying the described method for equal surfaces separately to both materials. For each of these symmetric systems, one obtains the midplane potential  $\Psi_m$  and thus via Eq. (17) the full potential function  $\Psi(x)$  associated with any given separation between equal plates. Since  $\Psi(x)$  is already fully determined by the value of  $\Psi_m = \Psi(0)$  and the requirement  $d\Psi/dx|_{x=0} = 0$ , solutions  $\Psi(x)$  of the Poisson-Boltzmann equation for different systems are identical if they correspond to the same  $\Psi_m$  (i.e. the same pressure), the only difference being the surface separation  $h$  for which they occur in the two systems. A solution  $\Psi(x)$  associated with a separation  $h_1$  in one system and with separation  $h_2$  in the second system clearly serves as a solution in a mixed system with a surface of type 1 at  $x = -h_1/2$  and a surface of type 2 at  $x = +h_2/2$ . Moreover, the separation  $h = (h_1 + h_2)/2$  at which this solution occurs in the mixed system is unique, because the pressure is a monotonic function of separation in the symmetric systems and can thus be inverted to give the two separation functions  $h_1(\Psi_m)$  and  $h_2(\Psi_m)$ . Our strategy therefore consists of computing  $\Psi_m$  for all separations of interest in the symmetric systems 1 and 2, finding the separations  $h_1(\Psi_m)$ ,  $h_2(\Psi_m)$  by inversion, and finally inverting their arithmetic mean  $h(\Psi_m) = [h_1(\Psi_m) + h_2(\Psi_m)]/2$  to

obtain  $\Psi_m(h)$  and all the ensuing properties of interest in the mixed system.

Some results of this type are shown in Fig. 3, where we have plotted the charge density of a glass or silica surface and the electrostatic pressure as it interacts with either its own kind or with a surface of the carboxyl or the sulfate type. At the chosen ionic strength of 1 mM and pH 6, the charge of the silica surface is seen to deviate significantly from its value in isolation (horizontal line and Fig. 2) up to separations of several screening lengths. Moreover, the nature of the second surface also has a profound effect not only on the strength of the

interaction, but also on the charging state of the silica. While all anionic surfaces will reduce the effective charge on silica upon approach, the rate at which they do so strongly depends on the amount and variability of their own charge. Neither of these dependencies are usually considered in the discussion of interaction measurements. A recent attempt to determine these ionization properties of silica experimentally with atomic force microscopy [39] has been limited to symmetric surfaces, and relies on model assumptions both for the charge regulation and for the strong van der Waals forces at short surface separations.

#### IV. CONCLUSIONS

We have seen that the apparent charge on glass and silica surfaces of low specific area in pure water can be understood in terms of a simple model that was originally developed and tested for high electrolyte concentrations. Model predictions for effective charge densities compare favorably with interaction experiments on highly diluted silica spheres in deionized water [17]. They also support a new kinematic explanation of spurious long range attractions between like-charged particles near a single glass wall [16].

The regulated charge of silica and glass surfaces near contact with a second anionic surface, as well as the strength of the interaction, has been calculated from an exact solution of the nonlinear Poisson-Boltzmann equation. In commonly encountered solution conditions, the charge regulation of silica was found to be effective at separations well beyond a Debye length. It also proves very sensitive to the chemical nature of the opposing surface. Although the additional presence of van der Waals forces makes a quantitative measurement of these effects difficult, they should certainly be accounted for in the interpretation of interaction experiments.

This work was supported by the National Science Foundation through Grant Number DMR-9730189 and by the Deutsche Forschungsgemeinschaft.

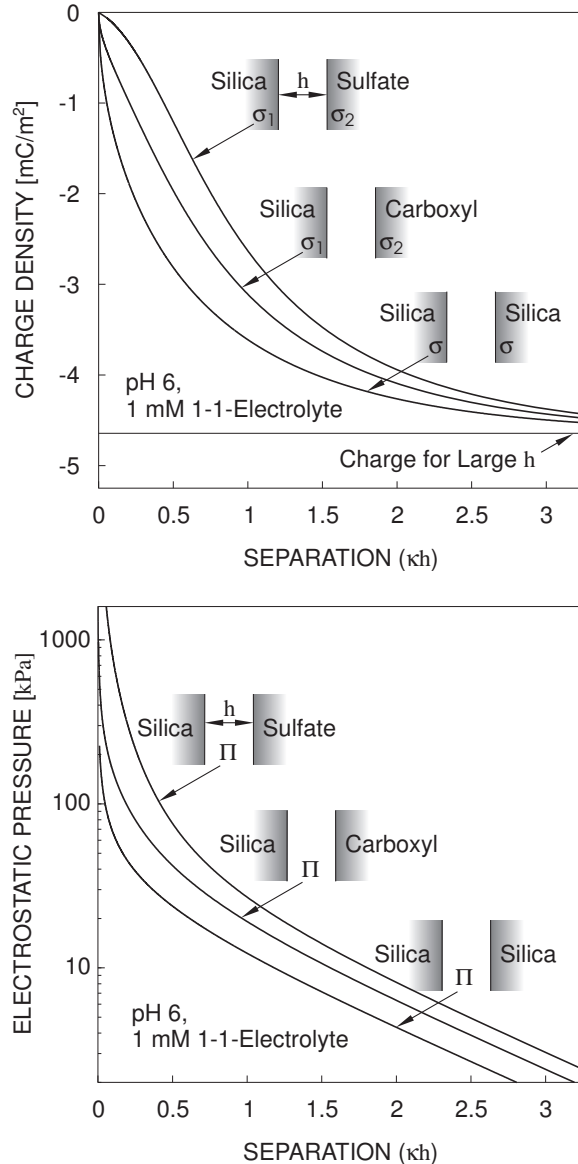


FIG. 3. The charge density of the silica surface and the force per unit area it experiences when interacting with any of the three presented types of surfaces at pH 6 and an ionic strength of 1 mM ( $\kappa^{-1} = 9.6$  nm). Surfaces parameters as in the previous figures.

- 
- [1] see, *e.g.*, M. Borkovec, B. Jönsson, and G. J. M. Koper in *Surface and Colloid Science*, **16**, 99–339, E. Matijević (ed.), Kluwer Academic / Plenum Press and references therein.
  - [2] R. K. Iler, *The Chemistry of Silica* (Wiley, New York, 1979).
  - [3] M. Kosmulski and E. Matijević, *Langmuir* **8**, 1060 (1992).
  - [4] R. S. Sanders, R. S. Chow, and J. H. Masliyah, *J. Colloid Interface Sci.* **174**, 230 (1995).

- [5] Y. G. Gu and D. Q. Li, J. Colloid Interface Sci. **226**, 328 (2000).
- [6] J. Yamanaka, Y. Hayashi, N. Ise, and T. Yamaguchi, Phys. Rev. E **55**, 3028 (1997).
- [7] L. A. Rosen and D. A. Saville, Langmuir **7**, 36 (1991).
- [8] M. Rasmusson and S. Wall, Colloids Surfaces A **122**, 169 (1997).
- [9] G. M. Kepler and S. Fraden, Phys. Rev. Lett. **73**, 356 (1994).
- [10] M. D. Carbajal-Tinoco, F. Castro-Román, and J. L. Arauz-Lara, Phys. Rev. E **53**, 3745 (1996).
- [11] J. C. Crocker and D. G. Grier, Phys. Rev. Lett. **77**, 1897 (1996).
- [12] A. E. Larsen and D. G. Grier, Nature **385**, 230 (1997).
- [13] J. E. Sader and D. Y. C. Chan, J. Colloid Interface Sci. **213**, 268 (1999).
- [14] J. C. Neu, Phys. Rev. Lett. **82**, 1072 (1999).
- [15] J. E. Sader and D. Y. C. Chan, Langmuir **16**, 324 (2000).
- [16] T. Squires and M. P. Brenner, Phys. Rev. Lett. **85**, 4976 (2000).
- [17] S. H. Behrens and D. G. Grier, Phys. Rev. Lett. submitted for publication (2001).
- [18] M. Elimelech, J. Gregory, X. Jia, and R. A. Williams, *Particle Deposition and Aggregation: Measurement, Modeling and Simulation* (Butterworth-Heinemann, Oxford, 1995).
- [19] H.-J. Butt, Biophys. J. **60**, 1438 (1991).
- [20] W. A. Ducker, T. J. Senden, and R. M. Pashley, Langmuir **8**, 1831 (1992).
- [21] D. C. Prieve, Adv. Colloid Interface Sci. **82**, 93 (1999).
- [22] S. H. Behrens and M. Borkovec, J. Phys. Chem. B **103**, 2918 (1999).
- [23] S. H. Behrens and M. Borkovec, Phys. Rev. E **60**, 7040 (1999).
- [24] T. Hiemstra, J. C. M. de Wit, and W. H. van Riemsdijk, J. Colloid Interface Sci. **133**, 105 (1989).
- [25] T. Hiemstra, P. Venema, and W. H. van Riemsdijk, J. Colloid Interface Sci. **184**, 680 (1996).
- [26] S. Alexander, P. M. Chaikin, P. Grant, G. J. Morales, P. Pincus, and D. Hone, J. Chem. Phys. **80**, 5776 (1984).
- [27] T. Gisler, S. F. Schulz, M. Borkovec, H. Sticher, P. Schurtenberger, B. D'Aguzzo, and R. Klein, J. Chem. Phys. **101**, 9924 (1994).
- [28] J. Westall and H. Hohl, Adv. Colloid Interface Sci. **12**, 265 (1980).
- [29] G. H. Bolt, J. Phys. Chem. **61**, 1166 (1957).
- [30] W. B. Russel, D. A. Saville, and W. R. Schowalter, *Colloidal Dispersions, Cambridge Monographs on Mechanics and Applied Mathematics* (Cambridge University Press, Cambridge, 1989).
- [31] H. Oshima, T. W. Healy, and L. R. White, J. Colloid Interface Sci. **90**, 17 (1982).
- [32] G. M. Bell, S. Levine, and L. N. McCartney, J. Colloid Interface Sci. **33**, 335 (1970).
- [33] A. de Keizer, E. M. van der Ent, and L. K. Koopal, Colloids Surfaces A **142**, 303 (1998).
- [34] B. W. Ninham and V. A. Parsegian, J. Theor. Biol. **31**, 405 (1971).
- [35] M. Abramowitz and A. Stegun, *Handbook of Mathematical Functions* (Dover, New York, 1972); I. S. Gradshteyn and I. M. Ryzhik, *Table of Integrals, Series, and Products* (Academic Press, San Diego, 1980).
- [36] See *e.g. Mathematica* (Wolfram Research Inc., Champaign, IL) or the *NAG Fortran Library* (NAG Ltd., Oxford).
- [37] S. H. Behrens *et al.*, Langmuir **16**, 2566 (2000).
- [38] S. H. Behrens, M. Semmler, and M. Borkovec, Prog. Colloid Polym. Sci. **110**, 66 (1998).
- [39] B. V. Zhmud, A. Meurk, and L. Bergström, J. Colloid Interface Sci. **207**, 332 (1998).